POSTERS

Experimental investigation on CO_2 methanation process for solar energy storage

B. Castellani, A. M. Gambelli, E. Morini, B. Nastasi, A. Presciutti, M. Filipponi, A. Nicolini, F. Rossi

ERASMUS +
IESRES
INNOVATIVE EUROPEAN STUDIES ON RENEWABLE ENERGY SYSTEMS

Introduction

The utilization of the captured CO_2 as a carbon source for the production of energy storage media offers a technological solution for overcoming crucial issues in current energy systems. Solar energy production generally does not match with energy demand because of its intermittent and non-programmable nature, entailing the adoption of storage technologies. Hydrogen constitutes a chemical storage for renewable electricity if it is produced by water electrolysis and is also the key reactant for CO_2 methanation (Sabatier reaction). The utilization of CO_2 as a feedstock for producing methane contributes to alleviate global climate changes and sequestration related problems. The produced methane is a carbon neutral gas that fits into existing infrastructure and allows to overcome issues related to the aforementioned intermittency and no-programmability of solar energy.

In this paper an experimental apparatus, composed by PV panels, an electrolyser and a tubular fixed bed reactor is built and used to produce methane via Sabatier reaction. The objective of the experimental campaign is the evaluation of the process performance and the comparison with other CO_2 valorization paths.

Methane and methanol production process

The two processes are shown in their schematic configuration, in witch are represented topical components of the production apparatus.

Scheme of the CO_2 methanation process.

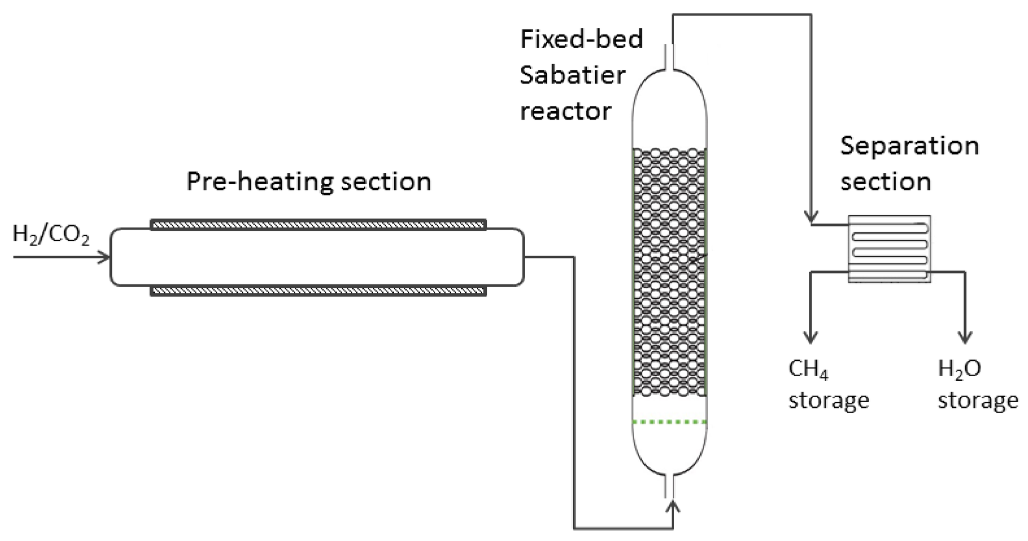

$$CO_2 + 4H_2 \rightarrow CH_4 + 2H_2O \qquad \Delta H = -165\ kJ/mol$$

The methane-based process is based on the trasformation of electrical energy to synthetic natural gas by means of an electrolyser and creating the conditions suitable for the Sabatier reaction. This reaction is exothermic and is limited by the thermodynamic equilibrium. Operating temperatures are typically around 250-400 °C.

Scheme of the methanol-based process.

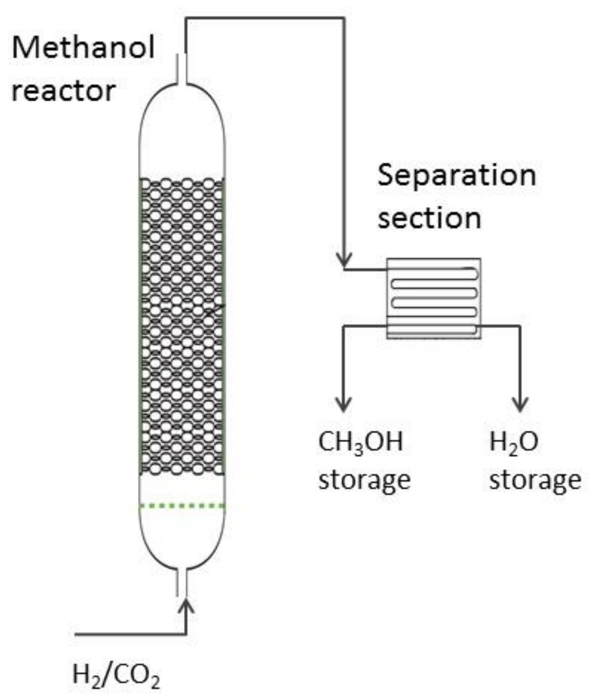

The reaction of conversion of CO_2 to CH_3OH is the following one:

$$CO_2 + H_2 \leftrightarrow CH_3OH + H_2O \qquad \Delta H = -49{,}5\ kJ/mol$$

The methanol production process is based on the use of hydrogen (also in this case it's produced by water electrolysis) in the conversion of electrical energy and CO_2. The reaction is highly exothermic therefore it's facilitated at high pressure and low temperature. CO_2 is converted to methanol in the ranges of temperature, 250-300 °C, and pressure, 5-10 Mpa using $CuO/ZnO/Al_2O_3$ catalyst. The produced methanol is liquid at ambient P and T and can be safely stored and handled.

Materials and methods

Experimental apparatus

The experimental apparatus includes the following sections: an electrolyzer, CO_2-H_2 mixing section, heating section, Sabatier reactor and a water separation section.

Experimental procedure

Hydrogen is produced by an electrolyzer, then it is mixed with CO_2 according to the stoichiometric proportion. Gas flows are controlled by flowmeters. The gaseous mixture flows throughs the two cameras; the first one constitutes the preheater section, while the second is the Sabatier reactor. The reactor is filled with Ni catalyst pellet, necessary for reaction development (it permits to improve the kinetics of the reaction). The reactor is equipped with one pressure sensor and ore temperature sensor (type K thermocouple). For reducing heat loss and for safety reasons, the two cameras are coated with thermo-insulating material.

Materials

The Sabatier reaction is catalysed by Ni-based catalyst containing oxide NiO. It has to be converted into the active form for the methanation reaction. Activation is achieved by the following process. At the beginning pure nitrogen is fluxed inside the reactor at 1.5 bar, in order to remove air present into the reactor. The internal temperature is brought to 220 °C with a rate of 60 °C/h. Then pure hydrogen is fluxed at 2 bar and the system is heated to 430 °C with a gradient of 120 °C/h.

Results and discussion

Experimental runs

The experimental campaign consists of 14 tests. The difference between one test and the other lies in the variation of four main parameters: CO_2/H_2 ratio, flow conditions, temperature and pressure. Values adopted for these parameters are shown in the following table.

Test	CO_2/H_2 Ratio	Batch or in-continuo (B-C)	Temperature [°C]	Pressure [bar]
1	1/4	C	250	2
2	1/4	C	317	2
3	1/4	C	363	4
4	1/4	C	490	4
5	1/4	C	422	8
6	1/4	C	451	20
7	1/4	B	250	10
8	1/4	B	271	10
9	1/4	B	350	10
10	1/4	B	353	15
11	1/1	C	371	16
12	1/1	C	325	17
13	1/1	C	329	17
14	1/1	C	378	17

Experimental tests were carried out with internal temperature in the optimal range from 250 °C to 451 °C and an internal pressure from 2 bar to 20 bar. Tests from 1 to 10 were carried out using the stoichiometric CO_2/H_2 ratio (1/4), while tests from 11 to 14 with ratio equal to 1. Only tests 7-10 were realized in batch conditions. For each test, the composition of the gaseous mixture collected at the end of the process is shown.

Test	*Pressure [bar]*	*Temperature [°C]*	*Final %v/v*		
			H_2	*CH_4*	*CO_2*
1	2	250	85.98	8.55	5.47
2	2	317	15.53	37.80	46.68
3	4	363	56.33	29.13	14.54
4	4	490	72.61	19.47	7.92
5	8	422	24.58	64.75	10.67
6	20	451	1.74	97.24	1.02
7	10	250	58.56	5.99	35.44
8	10	271	60.57	2.27	37.16
9	10	350	17.93	13.36	68.71
10	15	353	29.75	12.52	57.73
11	16	371	90.65	8.79	0.56
12	17	325	33.11	32.82	34.08
13	17	329	11.68	36.60	51.72
14	17	378	3.96	15.79	80.25

Discussion

Results allow to discuss the influence of the operating parameters on the methanation process. The in-continuo operation of the apparatus is clearly the fundamental element to obtain noteworthy results. Tests 11-14 demonstrated the strong conversion decrease caused by a deviation from the ideal value of the CO_2/H_2 ratio. Third place of importance is occupied by pressure, which accelerates the reaction and is directly proportional to the methane production rate. At the end, temperature represents an aid within its optimal range. The graphs clearly show the positive effect of pressure on the process, with an increasing regression line. Temperature instead has a beneficial action only within the range from 400°C to 450°C.

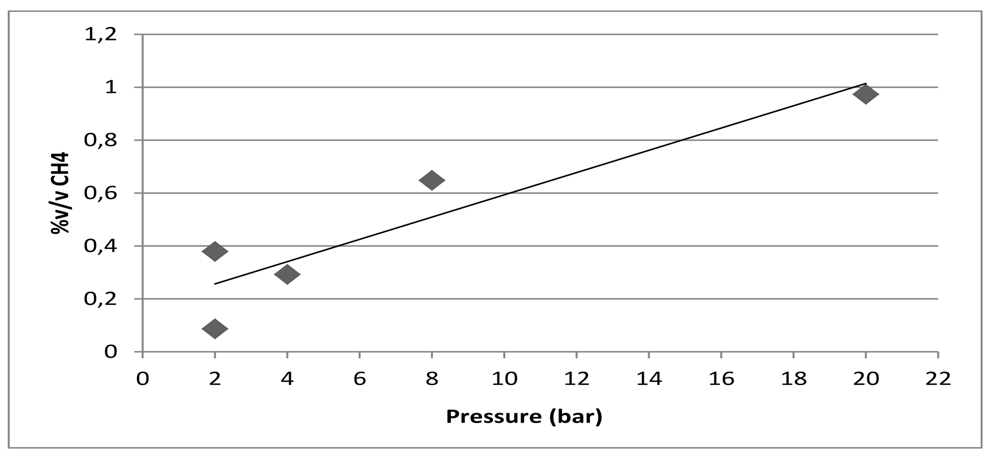

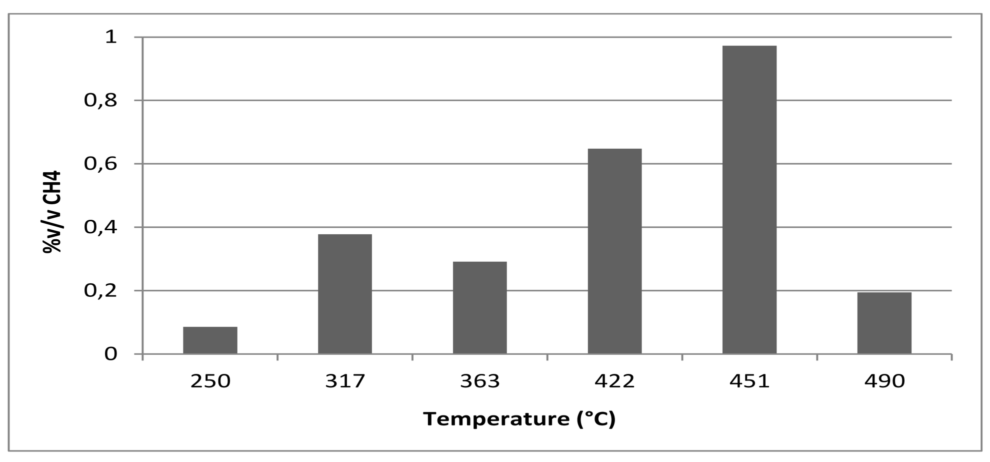

Comparison between methane and methanol production process

The experimental methane-based process was compared to the methanol-based process on the basis of the ratio: *Spent Energy/Stored Energy*. The considered parameter is an adimensional number calculated as the ratio between the specific energy spent in all the sections of the process to produce the fuel in its storing form and the pecific energy stored in the fuel. Process condition for both the processes are summarized in the following list.

Parameter	Methane process	Methanol process
Electrolyser working pressure (bar)	1	1
Synthesis reactor pressure (bar)	2	25
Synthesis reactor temperature (K)	573	493
Reaction heat (kJ/mol)	165	49
Conversion efficiency	0.9	0.9
Storage pressure (bar)	200	1
Storage temperature (K)	298	298

Then energy costs were calculated in accordance with parameters' values adopted in the previous list.

Energy consumption (kJ/kg_{fuel})	Methane process	Methanol process
Electrolyser	21115	10277
Gaseous mixture compression to synthesis pressure	2887	7593
reactor heating	10100	714
removal of reaction heat	3437	3437
Compression to storing conditions	1810	-
Total value	***39349***	***19097***

Results show that the ratio between the spent energy and the stored energy is higher for the methanol process. The methane production process has a best performance in terms of energy storage capability.

Acknowledgements: The authors are also grateful to European Union Ministry of Turkey, National Agency of Turkey Project Code: 2015-1-TR01-KA203-021342 entitled Innovative European Studies on Renewable Energy Systems.

Funded by the H2020 programme of the European Commission

Charging behavior of SiO_2 nano-electrets fabricated by electron implantation

Francesco Bonacci[1,2], Silvia Caponi [2], Francesco Cottone[1], Alessandro Di Michele[1], Maurizio Mattarelli[1]

[1]NiPSLab – Physics and Geology Department , University of Perugia

[2]IOM-CNR, Unità di Perugia, c/o Physics and Geology Department , University of Perugia

1 Introduction

Electret is a dielectric material that has a quasi-permanent electric charge or dipole polarization. An electret generates internal and external electric fields, and it is the electrostatic equivalent of a permanent magnet. Electrets have important technological application from established ones such as microphones or particulate filters to emerging ones as in **powering energy harvesting devices**. At smaller length scale a localized charge can improve the functionalities of nanostructured materials, providing further transduction schemes for **MEMS** and **NEMS** devices. However to guarantee the stability of the polarization in micro systems is challenging. Moreover, the fabrication process can induce significant changes in the structural and mechanical properties. In this work, we study the behavior of SiO_2 nano and microparticles when charged by injecting electrons by field emission scanning microscope (**SEM**) at energy ranging between 2 and 8 keV.

2 Charging process and electret fabrication by SEM

To asses the charging process we adopt the **Total Yield Approach** [1][2]

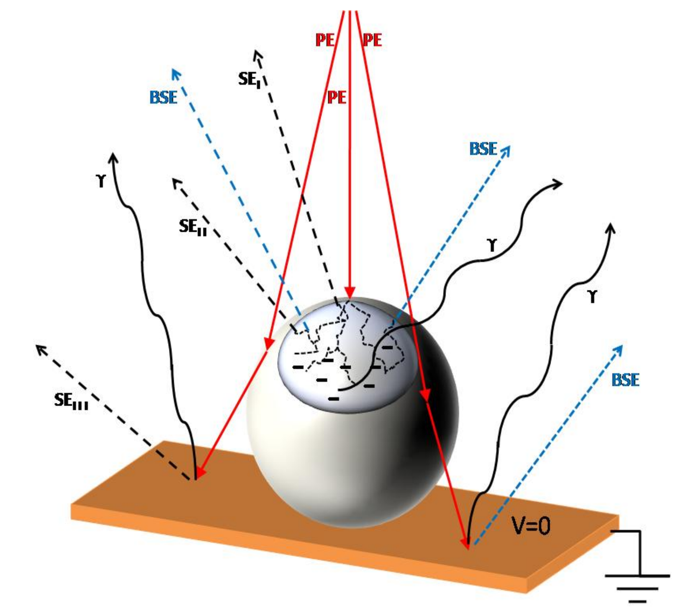

Fig.1 Interactions between the electron beam and the sample

We have different types of emitted particles:
1) Secondary electrons (SE)
2) Backscattered electrons (BSE)
3) X-ray

$$\delta = \frac{I_{SE}}{I_B} \qquad \eta = \frac{I_{BSE}}{I_B} \qquad \sigma = \delta + \eta$$

$$\frac{\partial Q}{\partial t} = (1-\sigma) I_B$$

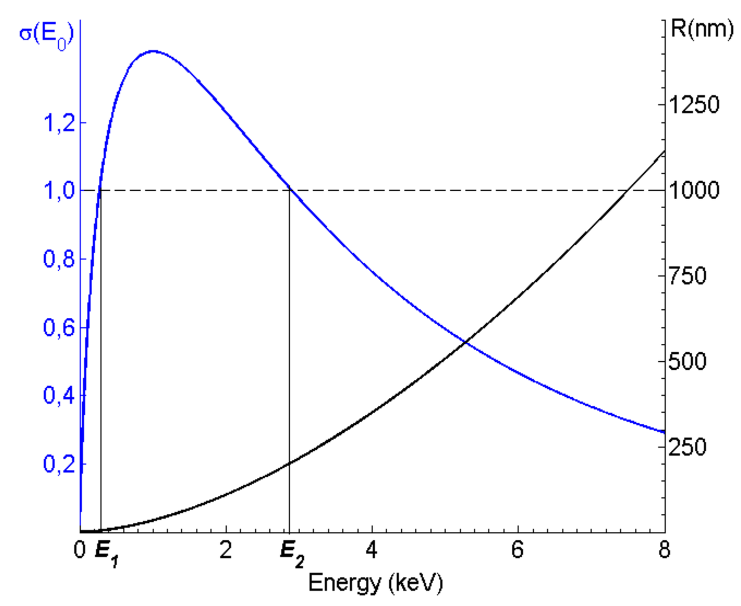

Fig. 2 Dependence of σ (total yield of emitted electrons) (blue line) and penetration depth R (black line) on beam energy

- There are three charging regions depending on the emission properties of the sample (**σ<1 or σ>1**)
- at the **crossover energy E_2** , the sample is uncharged
- Control on **penetration depth R ∝ $E_0^{1.67}$**

Increasing the primary electron energy, we expect to inject the charge deeper and deeper into the bulk of the material, leading the system to greater negative potential.

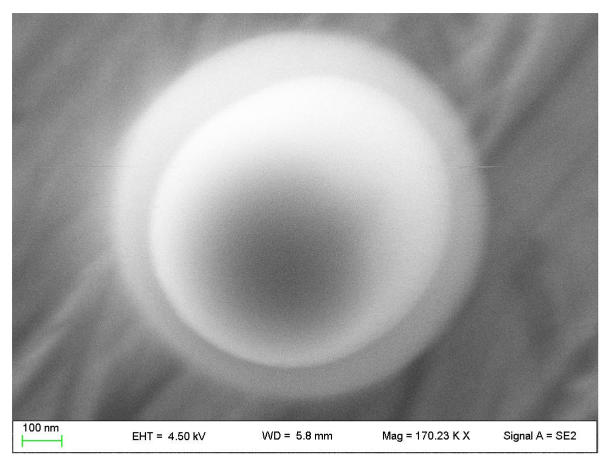

Fig. 3 Fabrication of the electrets by SEM. The bright region over the particle (due to enhanced SE emission) indicates the charge build up

3 Characterization of the charge by SEM

Shift of Duane-Hunt limit: The charge storage gives rise to a negative surface potential that has the effect to reduce the landing energy of the beam electrons.

$$E_L = E_0 - e|V_s| \quad \Rightarrow \quad e|V_s| = E_0 - E_L$$

The energy shift can be monitored measuring the **continuum x-ray radiation**: The energy cut-off of the spectra emitted from the charged region is compared with the energy cut-off of the spectra from a conductor at zero potential (expected to be E_0) [3]

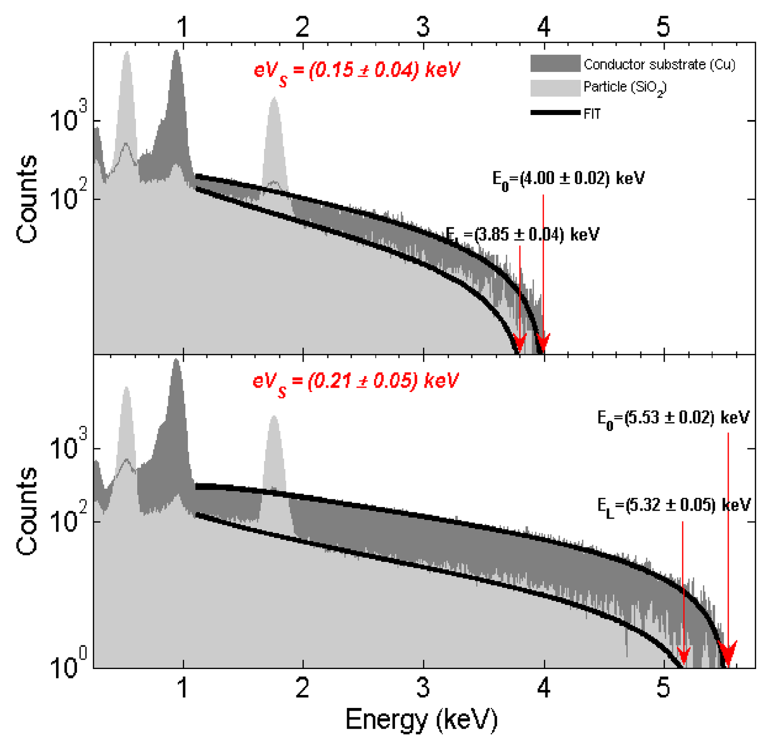

Electronic spectroscopy: The SEs energy distribution is shifted by the negative surface potential while its shape remains unchanged. [4]

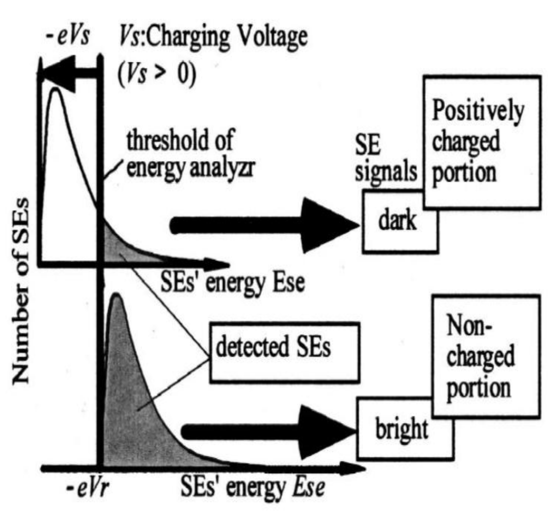

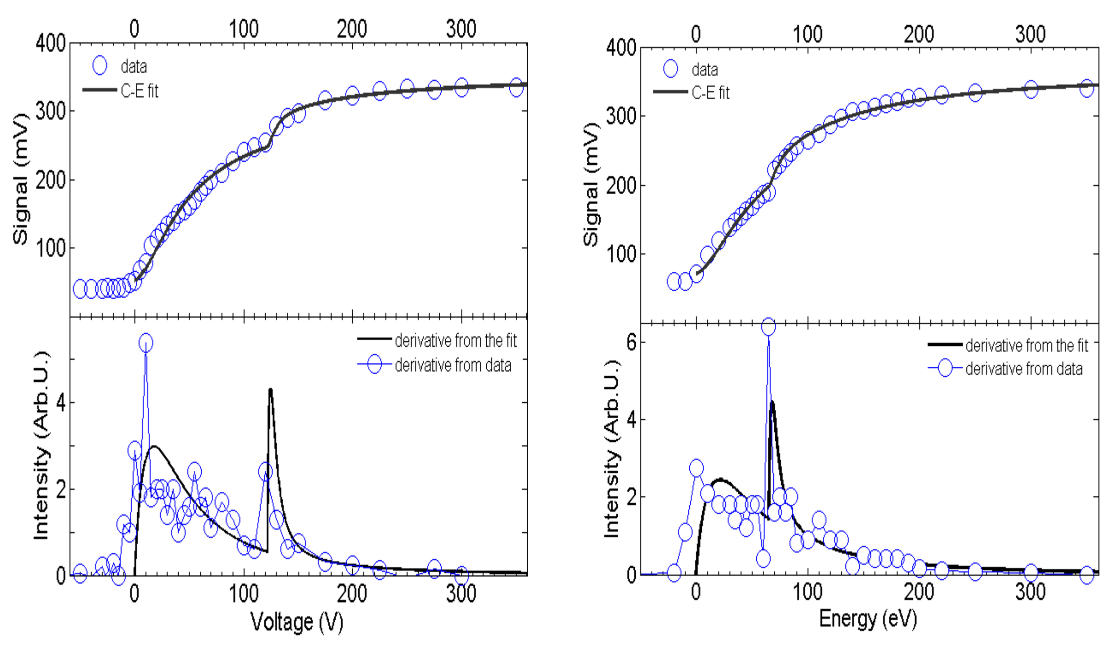

Changing the collector voltage V_c of the E-T detector we can select the energy of collected SEs.

SEs with higher kinetic energy (supplied by V_s) are detected at higher collector voltage V_c

4 Results

The measured surface potential is plotted as a function of the incident energy, both for 0.5 and 1.0 micron sized particles. We can see that in both cases the potential increases almost linearly at the beginning, until it reaches a maximum value and then become stationary, as there is a saturation due to the leakage and transmitted currents that prevent the dielectric breakdown. The maximum is reached when the penetration depth of the primary electrons is approximately equal to half the diameter of the particles. The measured surface potentials are consistent with those expected considering the dielectric strength of SiO_2

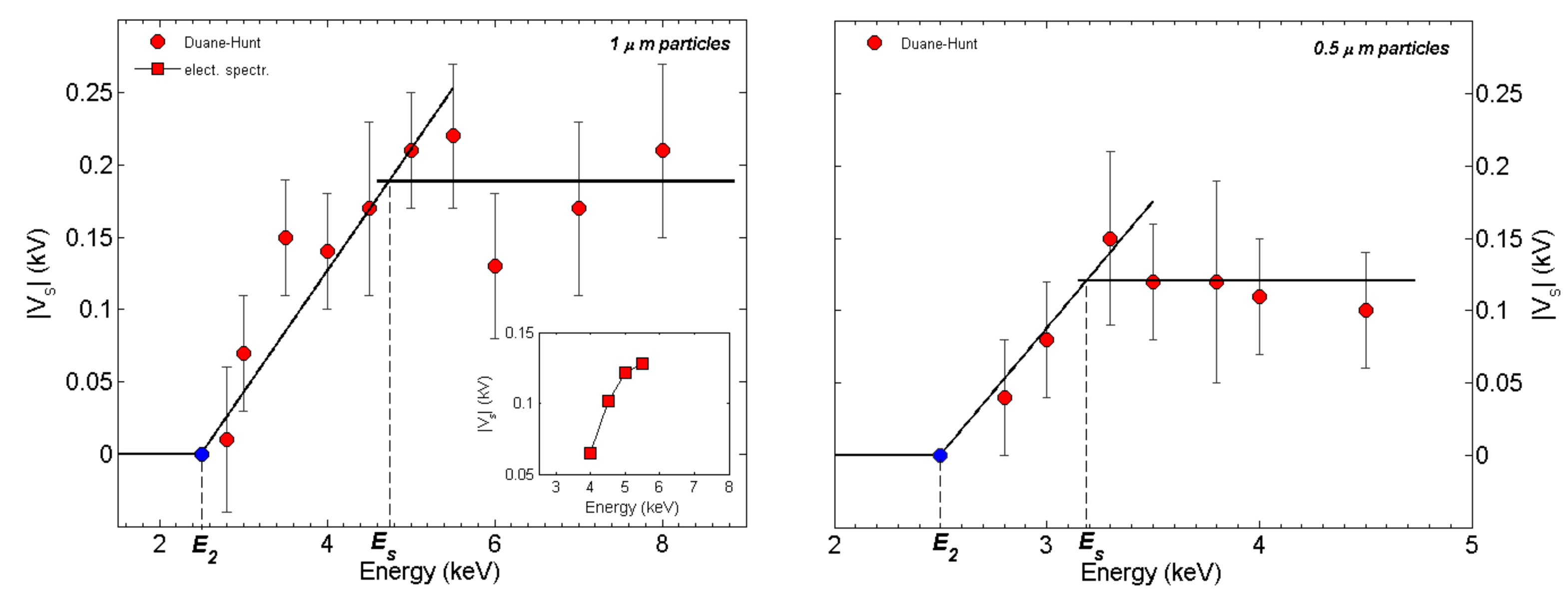

5 Time decay of the charge

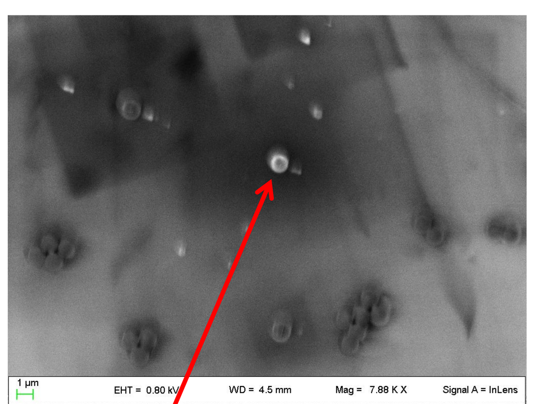

Charged particles are brighter

The charging state can be monitored by using SEM images collected at a much lower beam energy not to alter the pre-existing charge state.

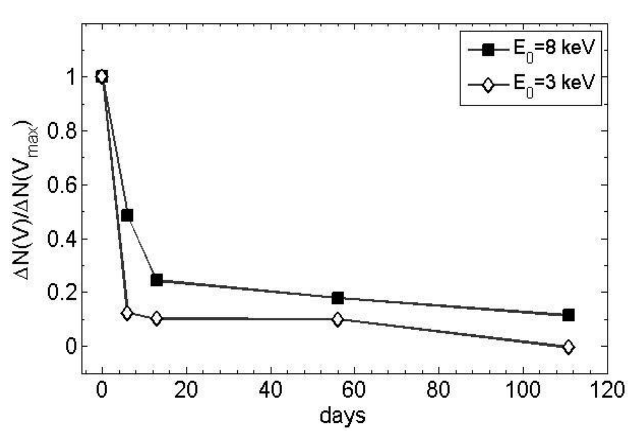

Two decay time constants:

- fast
- slow

6 Conclusion

In this work we have analyzed the behavior of micro and nanoparticles of SiO_2 exposed to an energetic electron beam, in order to fabricate electrets with reduced dimensionality. The values of the surface potential, acquired with two independent techniques, have shown that the particles have been charged till to the saturation level. The quite slow time decay allows exploiting them for new technological applications. It is also proved that SEM allows injecting efficiently the charge, and its high resolution allows controlling the penetration and the charging state of nano and micro structured samples.

References

[1] Cazaux. Scanning Vol. 26, 181–203 (2004)
[2] Thomson, Clint D. All Graduate Theses and Dissertations. Paper 2093
[3] M. Belhaj et al. Applied Surface Science 177 (2001) 58-65
[4] A. Takafuji et al. Microelectronic Engineering 61–62 (2002) 1083–1088

Acknowledgements

ERASMUS + : Innovative European Studies on Renewable Energy Systems (IESRES)

H2020: AdaPtative micROfluidic and nano-enabled smart systems for waTEr qUality Sensing (PROTEUS)

Fondazione Cassa di Risparmio di Perugia : Bando a tema Ricerca di Base 2016, Project Code: 2016.0106.021

Funded by the H2020 programme of the European Commission

Piezoelectric ZnO Microstructures: Synthesis and Characterization for Energy Harvesting

Giacomo Clementi, Francesco Cottone, Maurizio Mattarelli, Alessandro Di Michele, Silvia Caponi.
University of Perugia – Physics and Geology Department, via Pascoli, 06123 Perugia.

Introduction

In the last decade, zinc oxide (ZnO) has drawn attention for its characteristics as a smart material. One of its most studied properties is the ability to generate power when subjected to mechanical vibration. We synthesized ZnO microstructures on InterDigitated Electrodes (IDE) in order to obtain proof about their piezoelectricity and to develop microstruttured and well oriented microrods energy harvesters.

Modellization and Synthesis

Piezoelectricity is a natural property of certain materials to generate electric potential when they are subjected to mechanical stress. If a straight vertical rod is deflected, a strain field is created as the outer surface is stretched and the inner surface is compressed, resulting in an electric field along the z direction of the structure analysis. It's possible to estimate mechanical resonance frequency and piezoelectric potential by modeling, with finite element method (FEM), a ZnO microrod as a hexagonal structure and by applying a uniform horizontal force on its top surface (**Fig. 1**).

With hydrothermal route we obtained microrods on Si substrate and afterwards on IDE (**Fig. 2**). Solutions containing zinc acetate and HMTA (hexamine) yield rods with diameters of 3 ± 5 µm and lengths that range from 12 to 17 µm. The zinc acetate and HMTA concentrations should be 0.1M and 0.4M and the temperature of laboratory oven must be 85 °C, for 5h.

Resonance frequency:

$$\nu_n = \frac{\beta_n}{2\pi}\sqrt{\frac{EI}{mL^4}}$$

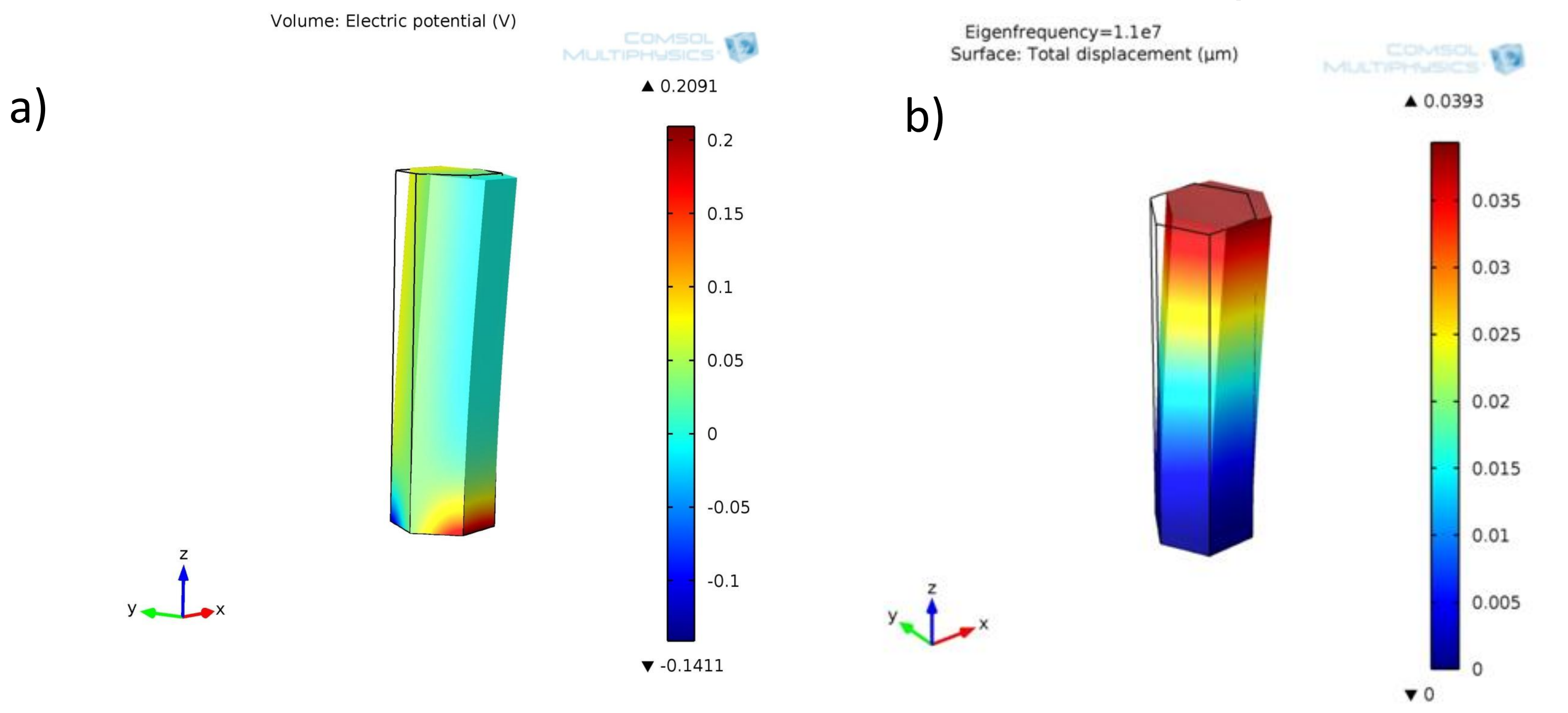

Fig 1: a) Electric Potential in a hexagonal rod generated by bending. b) First bending resonance frequency.

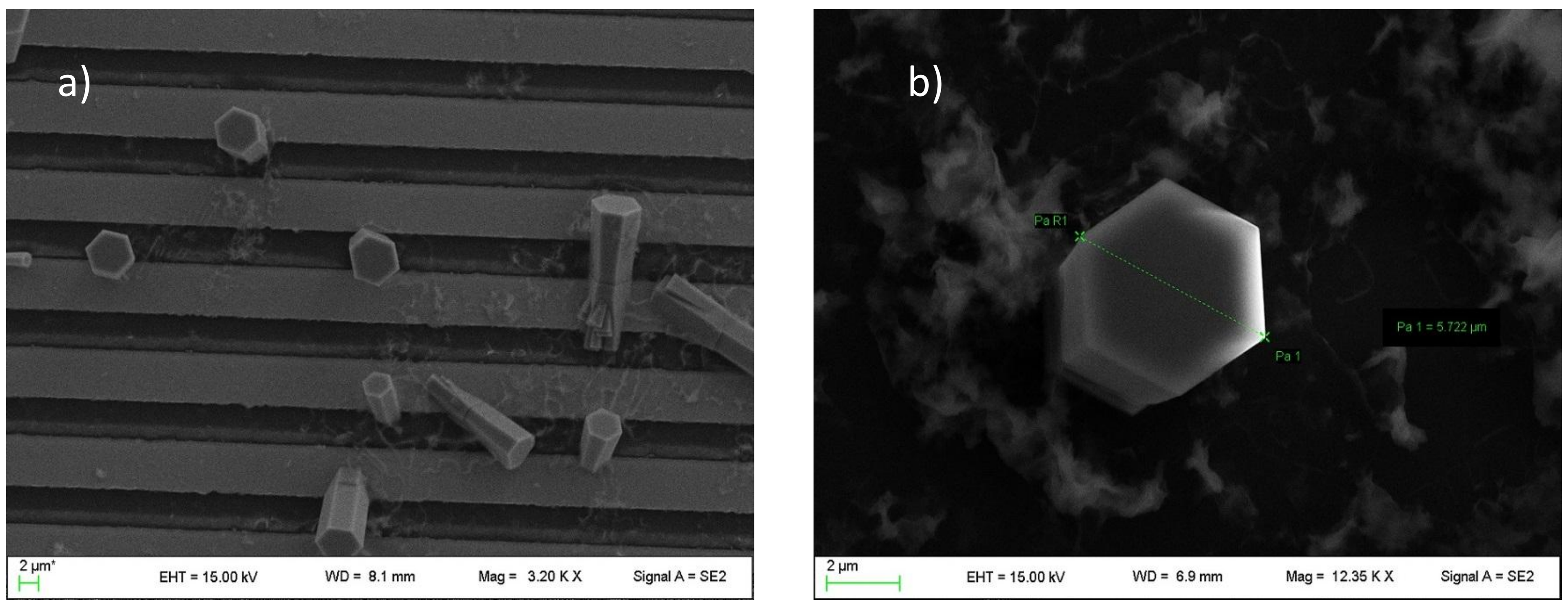

Fig 2: a) Microrods on IDE substrate. b) ZnO single crystal on Si substrate

Characterization

A scanning electron microscopy (SEM) with a field-emission-scanning electron microscope was used to observe the morphologies of ZnO microrods. Light scattering experimental techniques (micro-Raman and micro-Brillouin measurements on single crystal) were performed in order to estimate elastic and piezoelectric properties of microcrystals. X-Ray Diffraction (Cu Kα, λ= 1.5418 Å) gave us information about orientation of microrods on the substrate. SEM innovative method for piezoelectric characterization has been introduced: two conductive probes on a single crystal could give its mechanical frequency resonance driven by thermal noise.

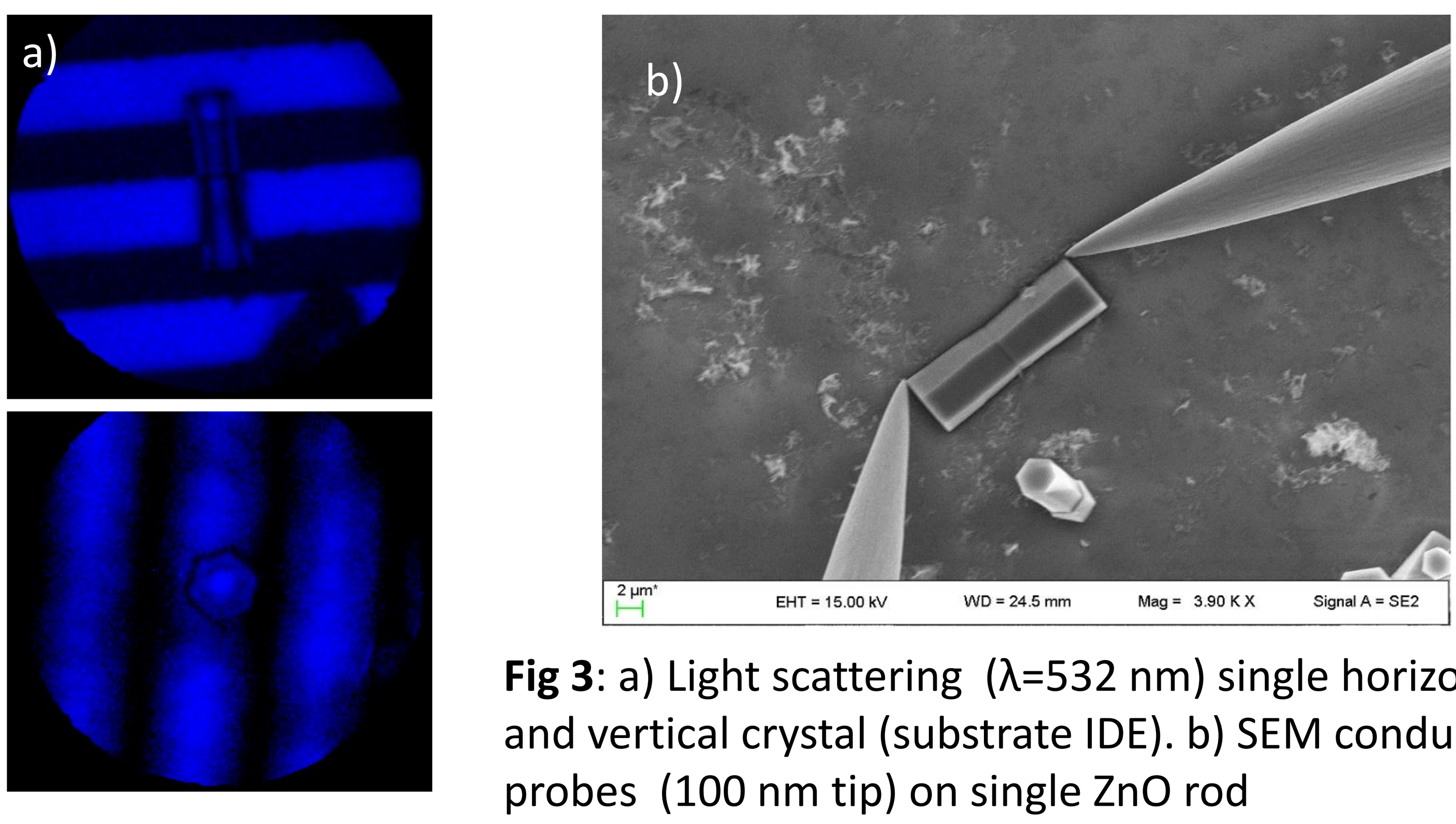

Fig 3: a) Light scattering (λ=532 nm) single horizontal and vertical crystal (substrate IDE). b) SEM conductive probes (100 nm tip) on single ZnO rod

Conclusion

ZnO microrods obtained by hydrothermal route could be studied to investigate their piezoelectric and elastic properties. Several techniques were used in this work, and a new one has been introduced, by using SEM conductive probes on a single crystal. In the near future we will continue to synthesize this micro materials on IDE with the aim to develop a device for energy harvesting from vibrational noise.

Acknowledgements

ERASMUS + : Innovative European Studies on Renewable Energy Systems (IESRES)
H2020: AdaPtative micROfluidic and nano-enabled smart systems for waTEr qUality Sensing (PROTEUS)

Funded by the H2020 programme of the European Commission

Results

•Light Scattering: Micro-Brillouin (Stiffness matrix elements **Tab.1**), Micro-Raman (Phonon modes of ZnO **Tab.2**)

•X-Ray Diffraction (Structure of microrods and their orientations)

•SEM probes on single crystal (Resonance frequency driven by piezoelectric effect and thermal noise)

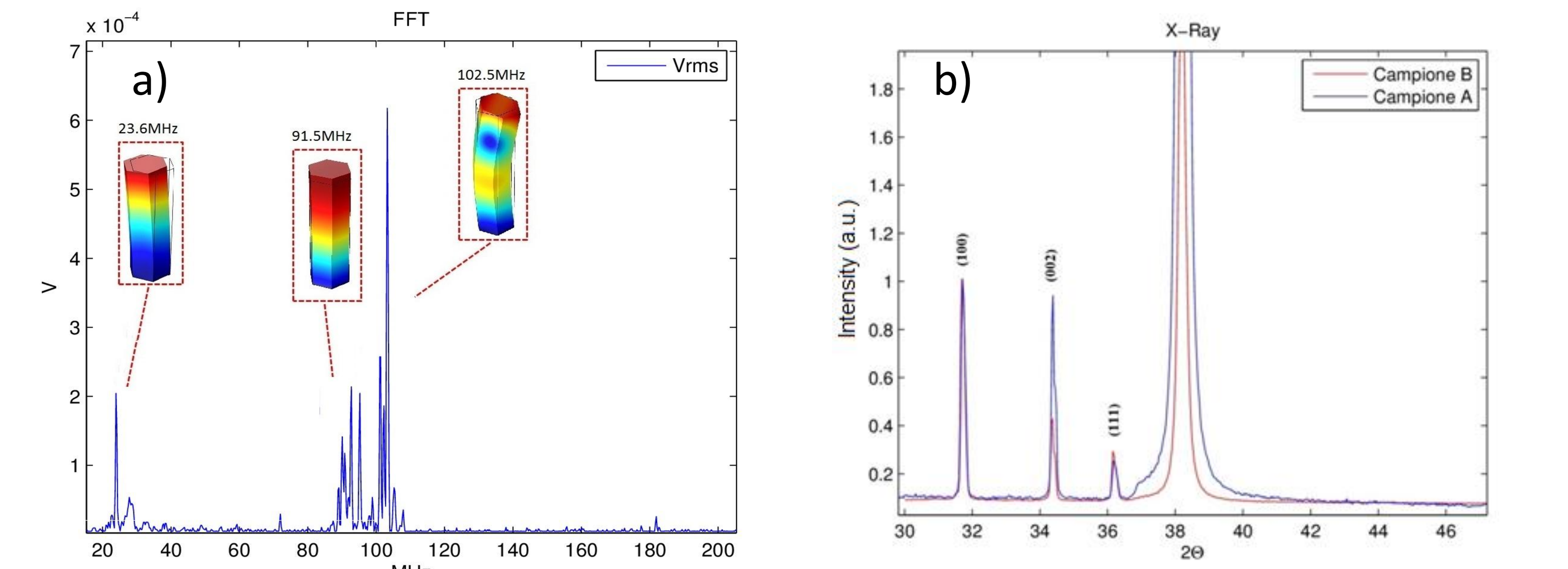

Fig 4: a) Resonance frequency (SEM probes on rod). b) X-Ray Diffraction on IDE

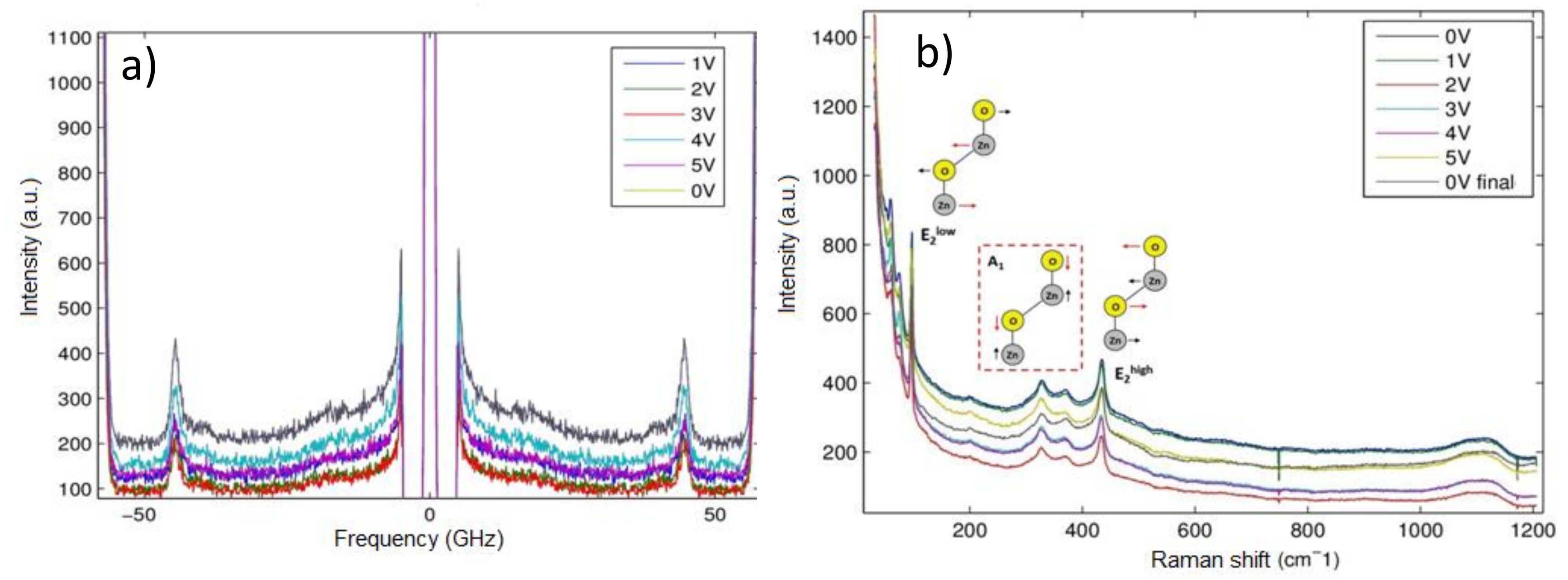

Fig 5: VV spectrum a) Micro-Brillouin on vertical crystal b) Micro-Raman on vertical crystal

Tab.1

Stiffness (GPa)	C_{11}	C_{33}	C_{44}	C_{66}
Ref. Bhat et al.	209	210	42	44
Results	209	198	42	43

Tab.2

Raman Shift (cm^{-1})	E_2^{low}	$A_1(E_2)$	$A_1(E_1,E_2)$	A_1	E_2^{high}
Ref. Damen et al.	101	208	332	380	437
Results	101	205	332	379	438

Yeni Bir Yüksek Manyetik Akı Yoğunluklu Elektromanyetik Üreteç*

Türkiye'nin merkezinde bir araştırma üniversitesi

Mustafa Melih Kale — (melihkale.58@gmail.com)
Sinan Akbaba — (snnkbb@gmail.com)

Elektrik Elektronik Mühendisliği Bölümü, Teknoloji Fakültesi, Gazi Üniversitesi, Beşevler, Ankara

Proje Akademik Danışmanı: Prof. Dr. Erol KURT (ekurt52tr@yahoo.com) *Sanayi Danışmanı:* Necmi ALTIN (SINE Enerji)

*Bu proje TÜBİTAK tarafından 2241/B SANAYİ ODAKLI LİSANS BİTİRME TEZİ DESTEKLEME PROGRAMI kapsamında 1139B411700171 kodu ile desteklenmiştir. Bu destekleri için TÜBİTAK'a teşekkür ederiz.

ÖZET

Bu proje kapsamında titreşim frekansları, 10 Hz - 30 Hz aralığında olan mekanik titreşimlerden elektrik üretmek için yeni bir elektromanyetik üreteç tasarlanıp üretilmiştir. Başlangıç olarak; Anysy Maxwell elektromanyetik benzetim paketi ile sistemin elektromanyetik modeli geliştirilmiş; yüksek yoğunlukta manyetik akı oluşturmak için nüve uçlarına Halbach metodolojisi ile eş kutuplu Neodiyum mıknatıslar yerleştirilmiştir. Sistem genel olarak; doğrusal laminasyonlu bir nüve yapısının etrafına sarılmış bir bobinden enerji üretimini konu almıştır. Nüvenin iki ucuna tutturulmuş iki yay yardımıyla geri çağırıcı kuvvet, basit harmonik hareket oluşturarak elektrik enerjisini açığa çıkarmaktadır. Sistemin sağlıklı çalışıp çalışmadığının tespiti için matematiksel formülasyonlar gerçekleştirilmiş, yenilikçi cihazın hem modeli ve elektromanyetik benzetimleri, hem de deneysel testleri tamamlanmıştır. Yapılan testlere göre yeni tasarlanan elektromanyetik enerji üreteci U = 0.75 V tepe gerilimi üretebilir şekilde maksimum P = 14 mW'lık elektrik gücü oluşturabilir biçimde tasarlanmıştır. Tasarlanan sistemin kablosuz ağlar, düşük güç üreten alarm sistemleri gibi alanlarda hareketin bulunduğu ortamda sürekli güç oluşturabilme yeteneği bulunmaktadır. Bu tür cihazlarda maksimum güç yoğunluğunu önemli bir parametre olup, P_V=0.3684 mW/cm³ değeri ülkemizde üretilen diğer üreteçlere göre çok iyi bir değerdir. Literatürdeki diğer çalışmalarla cihazımızın durumu karşılaştırılmış, patent başvuru süreci devam etmektedir. Uluslararası konferanslarda da bazı bulguları sunulmuş olan bu projeden yurtdışı yayın olarak da SCI indekli bir dergiye makale gönderimi yapılmış olup eser hakem incelemesindedir.

CİHAZIN ANALİTİK ve ELEKTROMANYETİK MODELLENMESİ

Şekil 1(a)'de cihazın Maxwell 3D benzetim programıyla modellemesi yapılmış ve Şekil1(b)'de gösterildiği şekilde sonlu elemanlar yöntemiyle elde edilen manyetostatik bulgulardan manyetik akı yoğunluğu (B) tespit edilmiştir. Nüve ve bobin geometrisi ve elde edilen akı bu tasarımla kararlaştırılmıştır. Nüve uçlarında hareket boyunca 0.75 T akı yoğunluğuna ulaşılmıştır.

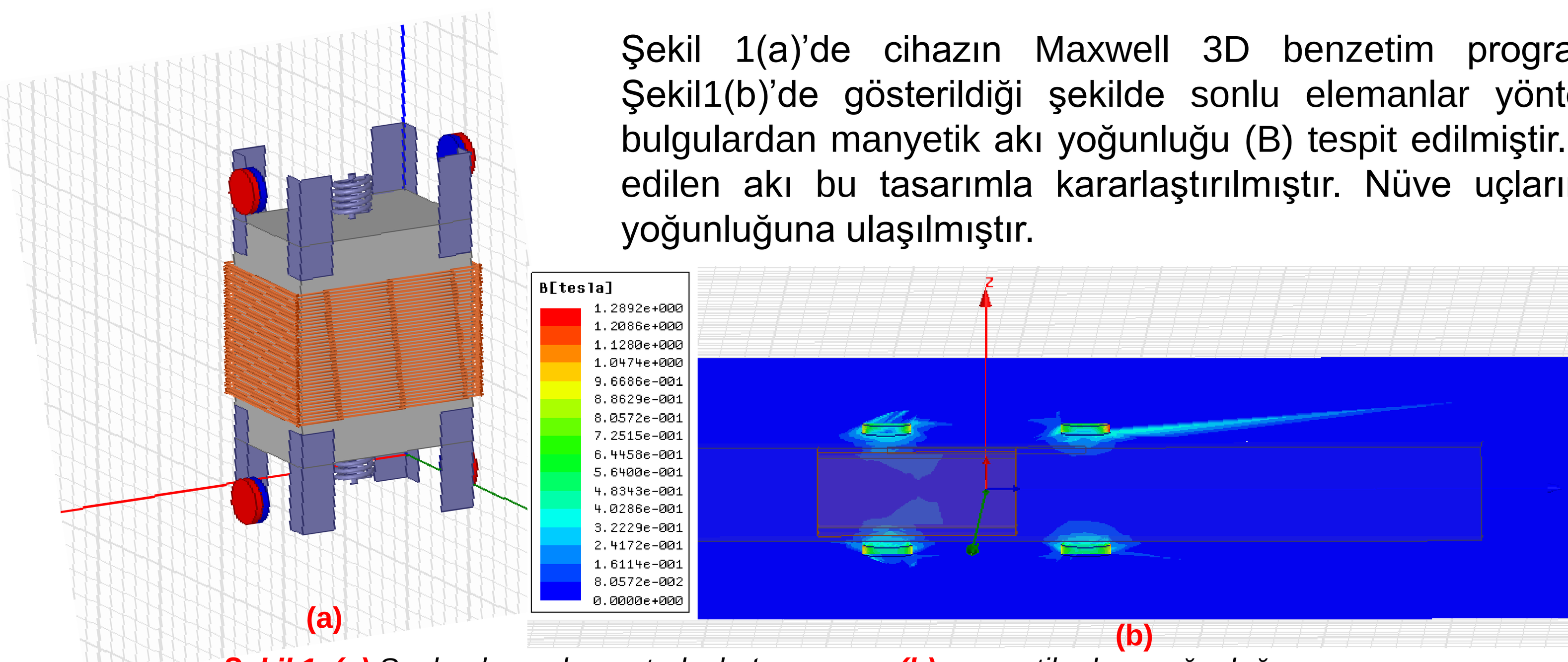

Şekil 1. (a) Sonlu elemanlar metuduyla tasarım ve (b) manyetik akım yoğunluğu

Analitik modelleme (Şekil 2(a)) ile cihazın cebirsel formülasyonları çıkartılmış, Maxwell benzetimi ile benzer sonuçlar akı yoğunluğu için elde edilmiştir. Şekil 2(b)'de cihazın titreşirken iki genel durumu ele alınmış olup azami ve asgari manyetik akı (Φ) durumları tespit edilmiştir.

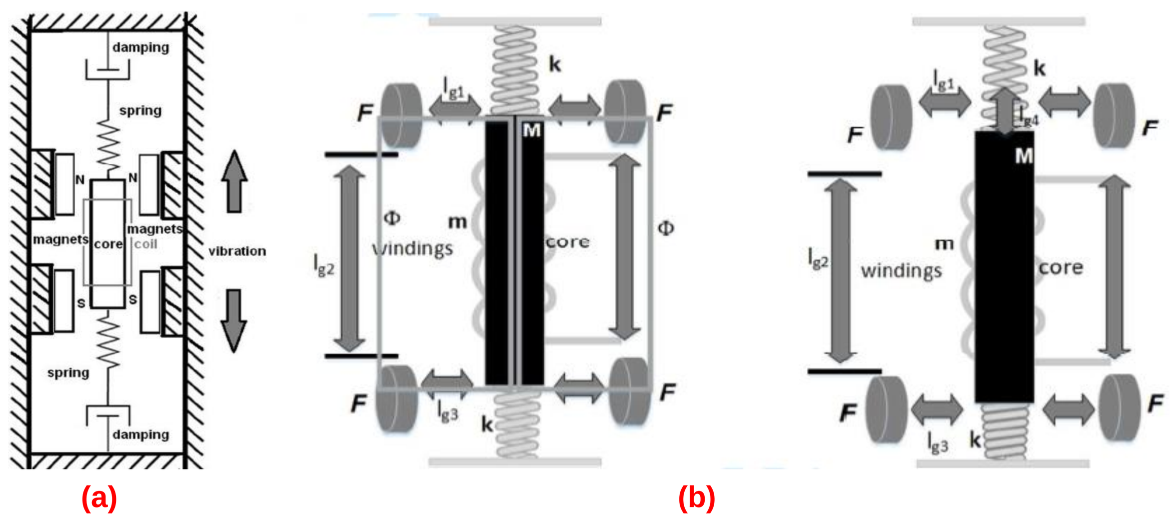

Şekil 2. (a) Analitik model ve (b) Φ manyetik akının asgari ve azami koşullardaki hesap metodu.

Analitik modellemede, cihazın titreşim halindeki hız ve kuvvet denklemleri ile manyetik akı ve Faraday denklemleri önem arzetmektedir:

$$v = \frac{dx}{dt} \quad (1)$$
$$(M+m)\frac{dv}{dt} + \gamma v + \omega_0 x = A\cos(\Omega t) \quad (2)$$
$$R_{tot}^{(1)} = R_{air}^{(1)} + R_{core}^{(1)} = \frac{2l_{g1}+l_{g2}}{\mu_0 A} + \frac{l_{g2}}{\mu_0\mu_r A} \quad (3)$$
$$\Phi = \frac{F}{R_{tot}} \quad (4)$$
$$\Phi^{(1)} = \frac{2F}{R_{net}^{(1)}} = \frac{2F}{\frac{2l_{g1}+l_{g2}}{\mu_0 A} + \frac{l_{g2}}{\mu_0\mu_r A}} \quad (5)$$
$$\Phi_{net}^{(1)} = 2\Phi^{(1)} = \frac{4F\mu_0\mu_r A}{(2l_{g1}+l_{g2})\mu_r + l_{g2}} \quad (6)$$
$$R_{tot}^{(2)} = R_{air}^{(2)} + R_{core}^{(2)} = \frac{2l_{g1}+l_{g2}+l_{g4}}{\mu_0 A} + \frac{(l_{g2}-l_{g4})}{\mu_0\mu_r A} \quad (7)$$
$$\Phi^{(2)} = \frac{2F}{R_{tot}^{(2)}} = \frac{2F}{\frac{2l_{g1}+l_{g2}+l_{g4}}{\mu_0 A} + \frac{l_{g2}-l_{g4}}{\mu_0\mu_r A}} \quad (8)$$
$$\Phi_{net}^{(2)} = \frac{4F\mu_0\mu_r A}{2\mu_R l_{g1} + l_{g2}(1+\mu_r) - l_{g4}(1-\mu_r)} \quad (9)$$
$$\Delta\Phi = \Phi_{net}^{(1)} - \Phi_{net}^{(2)} = \frac{4F\mu_0\mu_r A}{(2l_{g1}+l_{g2})\mu_r + l_{g2}} - \frac{4F\mu_0\mu_r A}{2\mu_R l_{g1} + l_{g2}(1+\mu_r) - l_{g4}(1-\mu_r)} \quad (10)$$
$$\Delta\Phi = \frac{-l_{g4}(1-\mu_r)4F\mu_0\mu_r A}{(2\mu_r l_{g1} + l_{g2}\mu_r + l_{g2})(2\mu_r l_{g1} + l_{g2}(1+\mu_r) - l_{g4}(1-\mu_r))} \quad (11)$$
$$\varepsilon = -\frac{d\lambda}{dt} \quad (12)$$
$$\lambda = N\Phi, \quad (13)$$
$$\varepsilon = -N\frac{d\Phi}{dx}\frac{dx}{dt} \quad (14)$$
$$\varepsilon = -Nv\frac{d\Phi}{dx} \quad (15)$$
$$\Delta\Phi = \frac{-x(1-\mu_r)4F\mu_0\mu_r A}{(2\mu_r l_{g1} + l_{g2}\mu_r + l_{g2})(2\mu_r l_{g1} + l_{g2}(1+\mu_r) - x(1-\mu_r))} \quad (16)$$
$$\frac{d\Phi}{dx} = \frac{-(1-\mu_r)4F\mu_0\mu_r A}{(2\mu_r l_{g1} + l_{g2}(1+\mu_r) - x(1-\mu_r))^2} \quad (17)$$
$$\frac{dx}{dt} = v \quad (18)$$
$$\frac{dv}{dt} = -\frac{\gamma v}{(M+m)} - \frac{\omega_0{}^2 x}{(M+m)} + \frac{A}{(M+m)}\cos(\Omega t) \quad (19)$$
$$\frac{d\Phi}{dx} = \frac{-(1-\mu_r)4F\mu_0\mu_r A}{(2\mu_r l_{g1} + l_{g2}(1+\mu_r) - x(1-\mu_r))^2} \quad (20)$$
$$\varepsilon = -Nv\frac{d\Phi}{dx} \quad (21)$$

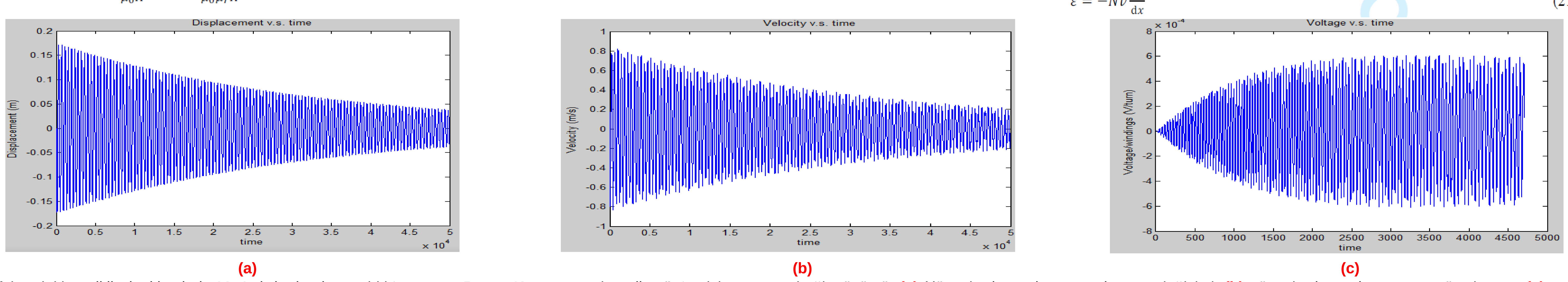

Şekil 3. Yukarıdaki analitik denklemlerin MatLab kodunda yazıldıktan sonra Runge-Kutta sayısal analiz yöntemiyle zamana bağlı çözümü: (a) Nüvenin denge konumundan yer değişimi, (b) nüvenin denge konumuna göre hızı ve (c) sarım sayısı başına üretilen gerilim.

Yukarıdaki denklemler MatLab paket program kodu halinde yazılarak yukarıdaki Şekil 3(a-c) gibi çözümler elde edilebilmektedir. Bu zamana bağlı çözümler bize ayrıca farklı parametre uzayını araştırma imkanını vermektedir. Şekillerden görüldüğü üzere, hız değişimlerinin yüksek olduğu ileri zaman çözümlerinde üreteçten üretilen gerilim artmaktadır. Bu da Faraday kanununu doğrular niteliktedir.

DENEYSEL ÇALIŞMALAR

Deneysel çalışmalar, bölümümüzde önceki TÜBİTAK projeleri ile kurulan Alternatif Enerji Araştırmaları Laboratuvarı ile Sine Enerji kurumunda gerçekleştirilmiştir. Şekil 4(a) bütün deneysel sistemi gösterirken imal ettiğimiz üreteç Şekil 4(b)'de ayrıntılı fotoğraflanmıştır. Bu sistem 1 Hz'den 50 Hz'e kadar yüksek frekans çözünürlüğünde sistemin titreşim frekansına bağlı davranışlarını test etmemize imkan vermektedir. Şekil 5(a-c)'de bu test sisteminden elde ettiğimiz örnek üç gerilim dalga formu ve eşlik eden nüve yer değiştirmesi gösterilmektedir. Görüldüğü üzere gerilim dalga formu tıpkı teorik çalışmadaki gibi yerdeğişimine çok bağlıdır. Deneyden ayrıca, dalga formunun sinüzoidal olmadığı görünmektedir. Ayrıntılı testler, sistemin doğal frekansı olan 16 Hz'de maksimum gücün elde edildiğini göstermektedir (Şekil 6(a)). Ayrıca; üretecin empedansına eşit yük ile gücün yüke maksimum iletildiği görülmüştür (Şekil 5(b)). Şekil 7'de üreteçten elde edilen gerilimin titreşim frekansına göre değişimini vermektedir.

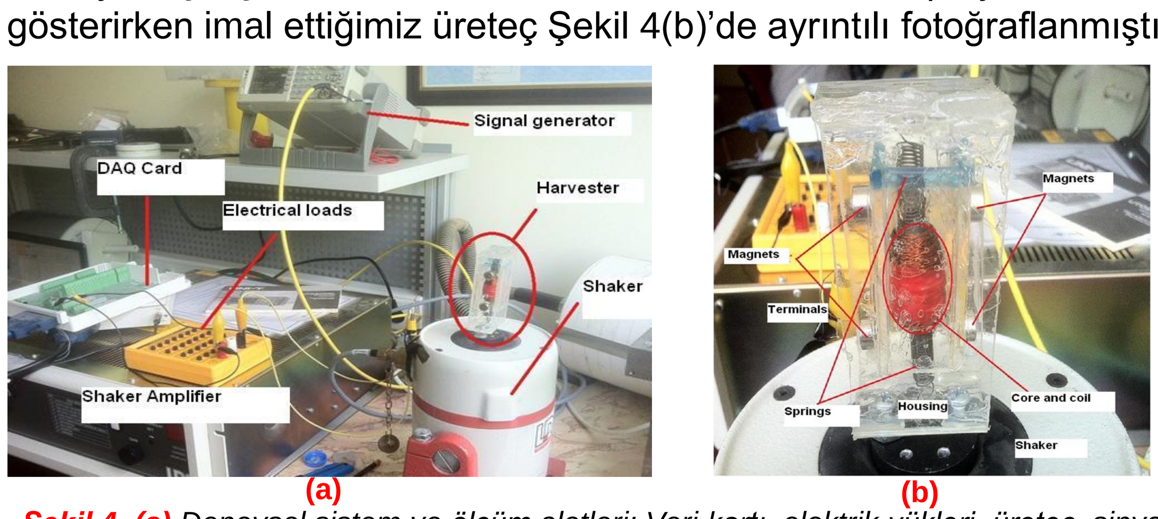

Şekil 4. (a) Deneysel sistem ve ölçüm aletleri: Veri kartı, elektrik yükleri, üreteç, sinyal jeneratörü, titreştirici amplifikatörü, titreştirici. (b) İmal edilen üretecin detay fotoğrafı

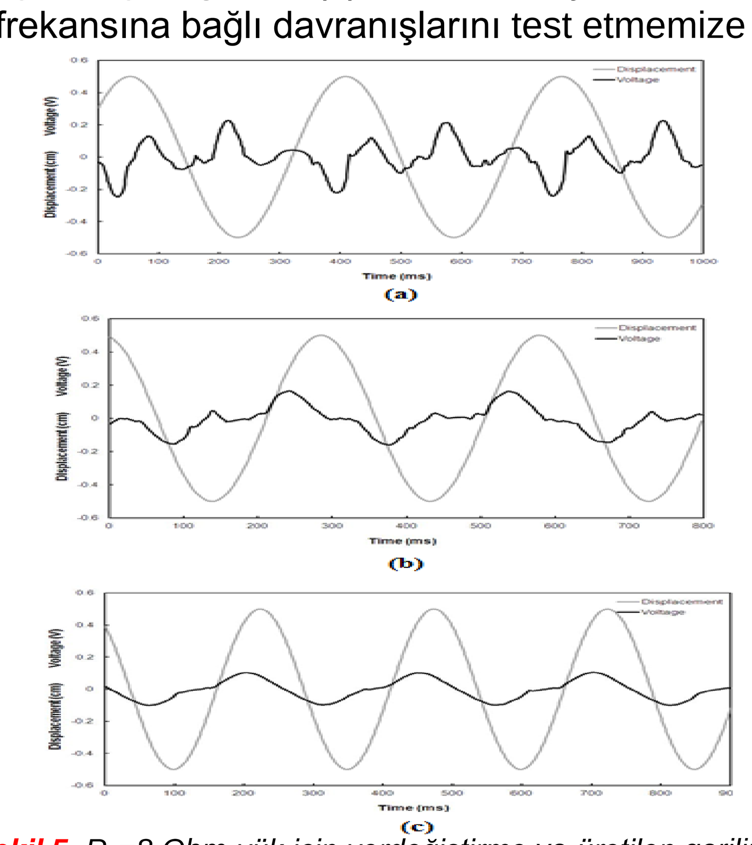

Şekil 5. R_L=8 Ohm yük için yerdeğiştirme ve üretilen gerilim dalga formları: (a) f=14 Hz, (b) f=17 Hz, (c) f=20 Hz.

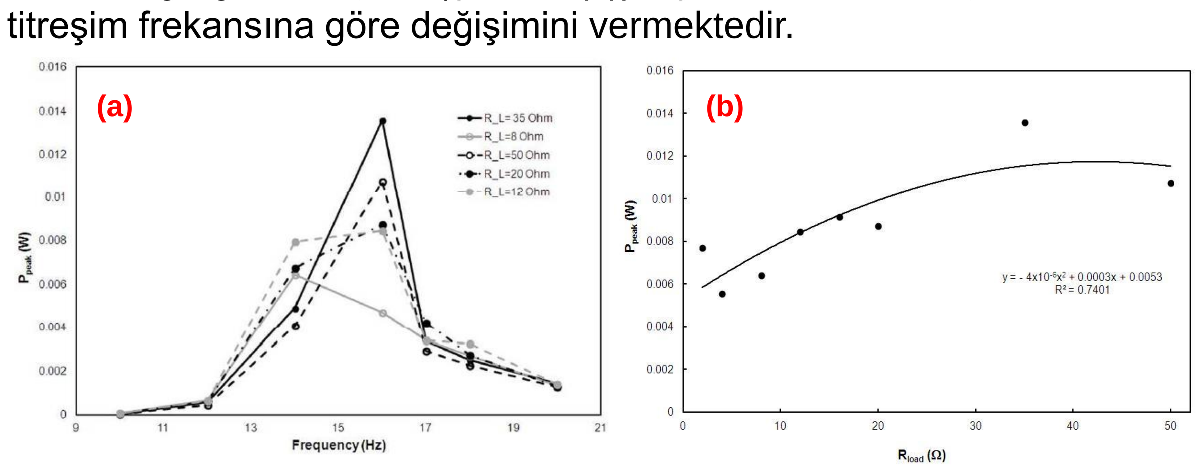

Şekil 6. (a)Farklı yükler için frekansa göre cihazdan maksimum elde edilen güçler. (b) Maksimum gücün elektriksel yüke bağımlılığı.

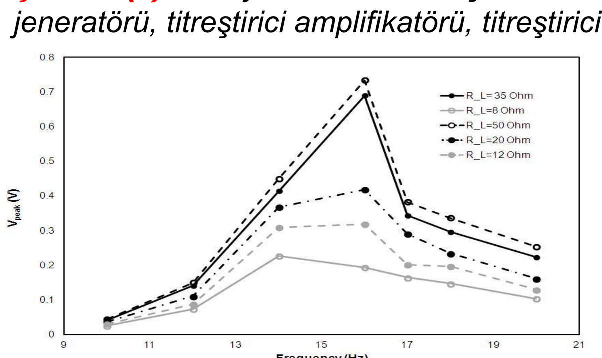

Şekil 7. Farklı yüklerde frekansa göre maksimum gerilim değişimi.

Literatürde 30 Hz'in altında maksimum gerilim elde edilen cihaz bütün dünyada çok azdır. Bu cihaz, 16 Hz gibi düşük frekansta maksimum gücü üretebilmektedir. Bu da cihazın kendi kadar yenilikçi bir özelliktir.

SONUÇLAR ve LİTERATÜR

- ✓ **Bu projeyle yenilikçi bir düşük güç enerji üreteci akademik ve teknolojik literatüre sokulmuştur.**
- ✓ **Cihaz dünya literatürüne göre gayet iyi güç yoğunluğuna sahiptir.**
- ✓ **Üretimi tamamen yerli olup en ucuzudur.**
- ✓ **Nüvenin 2,5 mm çalışma mesafesi için f = 16 Hz'de P = 16 mW tepe gücü üretebilmektedir.**
- ✓ **Optimum güç 40 Ω ' da elde edilmektedir.**
- ✓ **Yenilikçi cihaz için patentleme çalışması devam etmektedir.**
- ✓ **Uluslararası konferanslarda (*33. Türk Fizik Derneği Konf.* ve *5. Avrupa Yenilenebilir Enerji Sistemleri Konf.*) bulguların bir kısmı sunulmuştur.**
- ✓ **SCI indeksli yurtdışı dergisine makale olarak gönderilmiştir.**
- ✓ **Farklı prototiplerle güç yoğunluğunda en iyi olmak için çalışmalar devam etmektedir.**

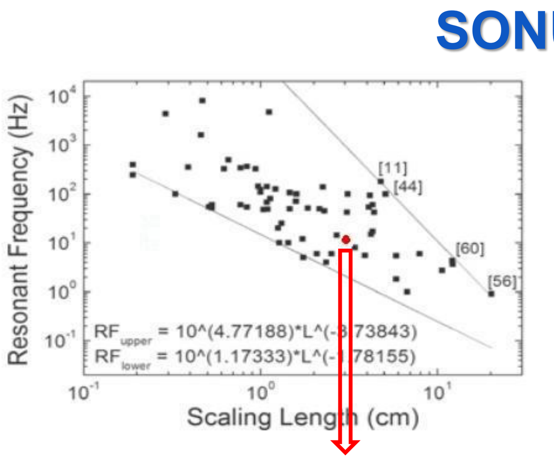

Alt teorik sınır en düşük frekansı temsil etmektedir. Dünyada bu sınıra büyük ölçekleme uzunluğuyla yaklaşan sayılı elektromanyetik üreteç bulunur. Onlardan birisi tasarladığımız üreteçtir.

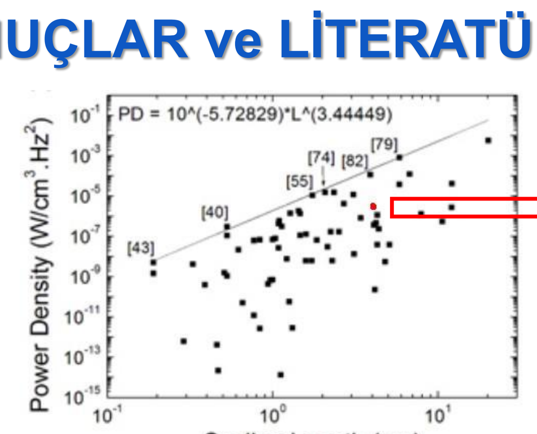

Üretecimizin, güç ve güç yoğunluğuna göre dünyadaki diğer elektromanyetik üreteçler arasındaki durumu. Ölçekleme uzunluğu cihaz hacminin küpkökü olarak tanımlanır.

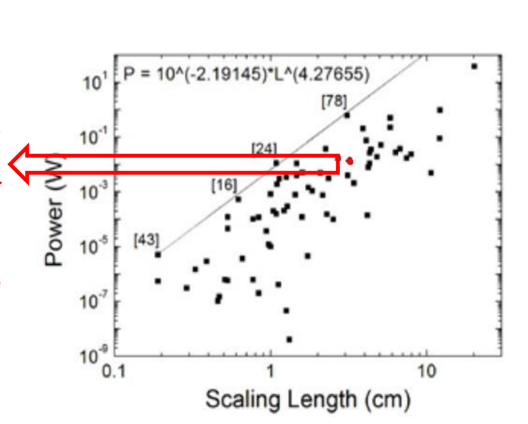

Üretecimizin, güce göre dünyadaki diğer elektromanyetik üreteçler arasındaki durumu. Hareketli kütleye göre.

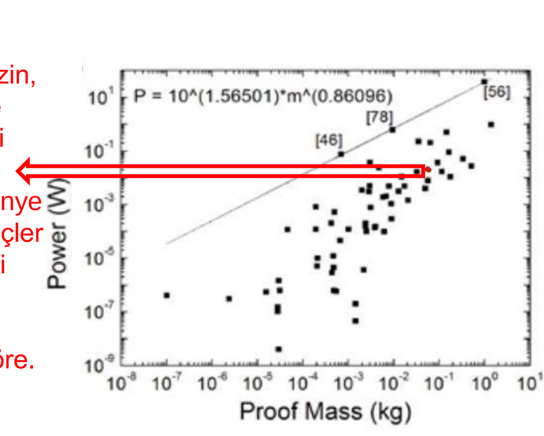

1. Kurt, E., Akbaba, S., Kale, M.M., «Analytical and experimental studies on a new linear energy harvester», **Canadian J. Physics**, under review, (2017).
2. Uzun, Y., & Kurt, E., «The effect of periodic magnetic force on a piezoelectric energy harvester», **Sensors and Actuators A: Physical**, 192, 58-68 (2013).
3. Uzun, Y., Kurt, E., Kurt, H.H., «Explorations of displacement and velocity nonlinearities and their effects to power of a magnetically-excited piezoelectric pendulum», **Sensors and Actuators A: Physical**, 224, 119-130, (2015).
4. Kurt, E., Gör, H., Demirtaş, M. «Theoretical and experimental analyses of a single phase permanent magnet generator (PMG) with multiple cores having axial and radial directed fluxes», **Energy Conversion and Management**, 77, 163-172, (2014).
5. Spreemann, D., & Manoli, Y. «Electromagnetic vibration energy harvesting devices: Architectures, design, modeling and optimization (Vol. 35)» Springer Science & Business Media, (2012).
6. Amirtharajah, R., & Chandrakasan, A. P., «Self-powered signal processing using vibration-based power generation», **IEEE J. Solid-state Circuits**, 33(5), 687-695, (1998).

Underwater piezoelectric energy harvester

Maurizio Mattarelli, Francesco Orfei and Francesco Cottone
Department of Physics, University of Perugia, Perugia, Italy

***Abstract*— In this works we present an energy harvester for underwater applications. It is based on a piezoelectric cantilever and it can be used to harvest energy in water pipelines. We present a finite elements analysis and the experimental results of the tests conducted in a reduced size model of a real pipeline.**

I. INTRODUCTION

In this paper we describe how we are powering a sensor to monitor physical and chemical parameters in a water pipeline. In order to provide self-powering capability to wireless sensor devices, we decided to not use batteries but an energy harvester [1, 2]. Generally, a turbine (e.g. Pelton, Darrieus) for capturing the energy of the water flux is used, but we have chosen to exploit the vibrations induced by the Von Karman Vortex [3] generated by turbulence around a cylindrical or blunt body.

Fig. 1 shows a simulation of the vortex that a blunt body generates in a water flux. Self-sustaining drag and transversal lift force are generated by the vortex and after a transient the excitation becomes periodic.

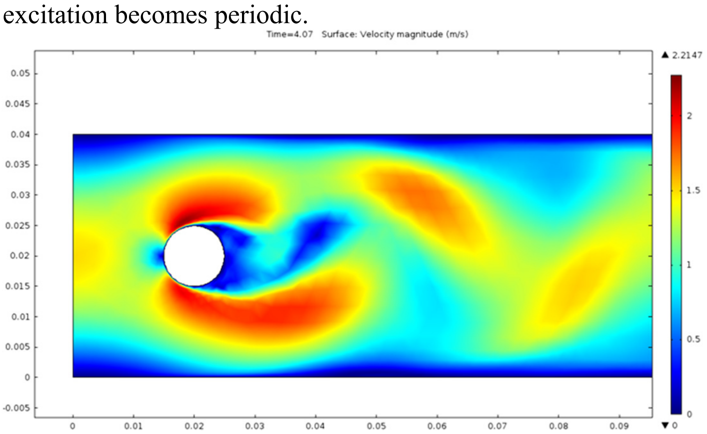

Fig. 1. 2D numerical simulation of water flux around a blunt body in a turbulent flow.

The work done by the vibrating lift force is converted into electricity by using a piezoelectric element. This way to harvest energy presents some advantages versus micro turbines:

- independent from flow direction;
- self-starting and reduced maintenance;
- small reduction of the flow pressure (1/100 bar);
- capacity to avoid solid bodies or particulate present in waste or rain water;
- no need of flow constraint.

II. ENERGY HARVESTER DESIGN

The first version of the water flux energy harvester is based on piezoelectric element, thus we named it Piezoelectric Vortex Generator (PVG). The overall mechanical design of the generator is shown in Fig. 2.

The transduction element is a bimorph piezoelectric beam that is provided by Midé Volture company (www.mide.com, model V21BL). Two piezoelectric layers are deposited on the side of inner steel layer and have copper electrodes on both sides. Then the beam is packaged with FR4 and presents a thickness of 0.8 mm. The mechanical water-air interface is disk-cap printed in ABS. This element has the important function of feedthrough for electrical connections.

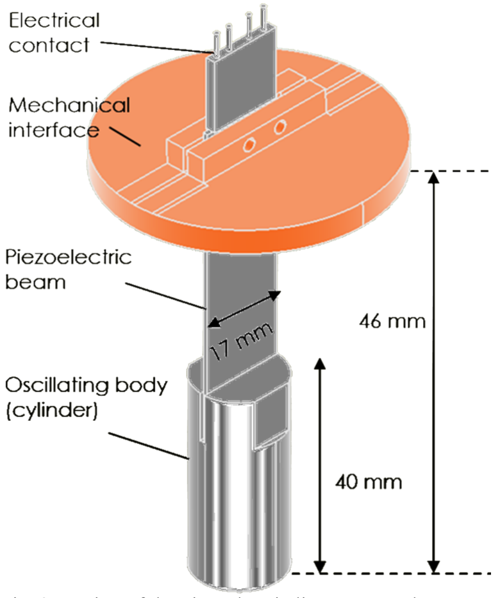

Fig. 2. Design of the piezoelectric linear energy harvester.

This energy harvester works in linear mode and its resonance frequency, when in the water, is about 30 Hz. The excitation due to the water flux is a sinusoidal force at the frequency $f = St \cdot v/d$, where St is the Strouhal number [4], v is the speed of the water and d is the cylinder diameter. At the speed of 0.7 m/s, this corresponds to a frequency of 6 Hz. Even if the two frequencies are different, we obtained a good conversion confirming that our harvesting is working on a wide band.

III. TEST SETUP

In our lab at NiPS we have built a reduced scale (1:10) water circuit in order to test the energy harvester (Fig. 3). A pump pulls and pushes the water from a reservoir through a 2 inches wide pipeline where we placed the piezoelectric generator (PVG). Smaller flexible tubes (1 inch in diameter, in yellow) connect the test pipeline (in grey) to the pump and to the reservoir creating a closed loop circuit.

The pump is a common one for water. It is made by Lowara, model CEAM 80/5 A. It can provide a flux of 100 ltr/minute, requiring a power of 0.75 kW at 230 Vac. We also provided a power regulator to change the rpm of the pump and the flux of the water.

Our target is to make this system work with a flux of about 100 ltr/s: we can expect much more power in a real scenario. Thus this setup is useful to understand the capability of such kind of energy harvesters.

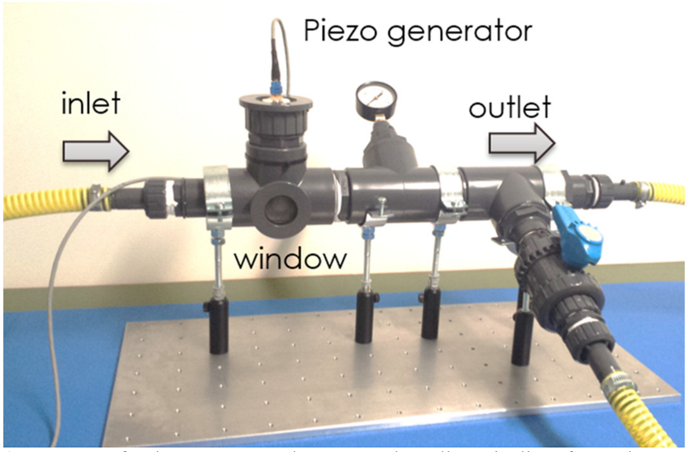

Fig. 3. Test setup for the PVG energy harvester. The yellow pipelines form a loop where the water flows from a reservoir through the piezoelectric generator to the reservoir again.

IV. PRELIMINARY RESULTS

We conducted several tests to evaluate our system. First, we investigated if the water flux was enough to make our generator to oscillate. After this we tried to optimize the depth of insertion of the oscillator in the pipeline. We performed this operation empirically trying to find the maximum output voltage with an oscilloscope.

Finally we evaluated the amount of power that can be converted in a typical working condition where the water flux was travelling at the speed of 0.7 m/s. We loaded the piezoelectric with a variable resistor and we have found that the optimal load value is 300 kOhm. In these conditions the RMS value of the output voltage is approximately 7 V and the corresponding power is about 160 μW.

Fig. 4 depicts the output voltage when the piezoelectric is loaded with a 300 kOhm resistor. As it can be seen, this signal is not sinusoidal. This is due to the impacts of the cylinder on the internal walls of the pipeline.

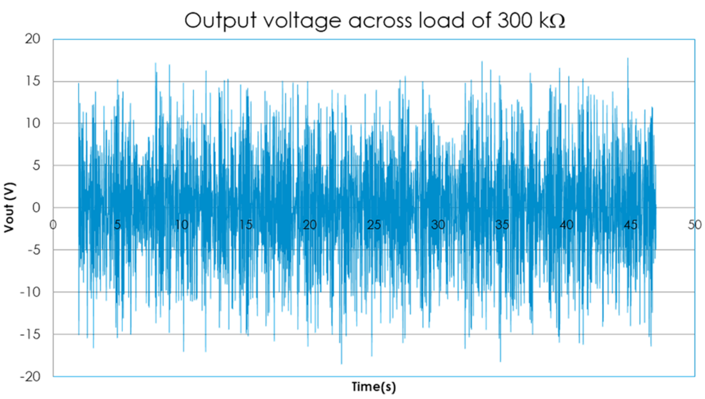

Fig. 4. Output voltage from the piezoelectric energy harvester when connected to a 300 kΩ load resistor.

V. CONCLUSIONS

We have demonstrated an alternative technology to extract energy from a water flux with minimal impact on the pressure in the pipeline (0.01 bar drop).

We have also demonstrated that Von Karman Vortex can be used to make extract energy from a flux by using a piezoelectric and that this energy harvester has a wide frequency response.

The proposed system can be further optimized: e.g. experimenting different shapes of the submersed oscillating body.

We are also working on self-tuning of the mechanical resonance frequency of the energy harvester with excitation: water speed can change and consequently the frequency of the excitation.

ACKNOWLEDGMENTS

This work is part of the research activities funded by the European Union (EU) Horizon 2020 Programme for research, technological development and demonstration (Grant agreement n. 644852, PROTEUS) and by The Ministry for European Affairs-National Agency of Turkey under the Grant No: 2015-1-TR01-KA203-021342 – IESRES.

REFERENCES

[1] Energy Harvesting Technologies, Shashank Priya, Daniel J. Inman, Spinger ISBN: 978-0-387-76463-4 (Print) 978-0-387-76464-1 (Online)

[2] Luca Gammaitoni, There's plenty of energy at the bottom (Micro and nano scale nonlinear noise harvesting), Contemporary Physics Vol 53 (2) Pages 119-135, 2012.

[3] Theodore von Kármán, Aerodynamics. McGraw-Hill (1963): ISBN 978-0-07-067602-2. Dover (1994): ISBN 978-0-486-43485-8.

[4] Strouhal, V. (1878) "Ueber eine besondere Art der Tonerregung" (On an unusual sort of sound excitation), *Annalen der Physik und Chemie*, 3rd series, **5** (10) : 216–251.